Vrublevsky A. V., Boshchenko A. A., Bogdanov Yu. I., Saushkin V. V., Shnaider O. L.
Research Institute of Cardiology, Tomsk National Research Medical Center of the Russian Academy of Sciences, Tomsk, Russia

Structural and Functional Disturbances of the Thoracic Aorta in Atherosclerosis of Various Gradations

Aim	To study global aortic circumferential strain in normal conditions and in atherosclerosis of various grades and to determine its role in prediction of structural and functional disorders of the thoracic aorta (TA) and coronary atherosclerosis using 2D speckle-tracking transesophageal echocardiography.
Material and methods	182 patients with typical or probable angina were examined. The control group consisted of 11 healthy volunteers. TA was visualized along its entire length. The height of each atheroma was measured, and the total number of plaques in the TA was determined. Five stages of TA atherosclerosis were identified. In the descending TA, the global peak systolic circumferential strain (GCS, %) and the global peak systolic circumferential strain normalized to pulse arterial pressure (PAP) (GCS/PAP·100) were calculated. All patients underwent coronary angiography. The number of coronary arteries (CAs) with >50% stenosis was determined, and the SYNTAX Score was calculated.
Results	TA atherosclerosis was not detected in the control group. Among 182 patients, stage 1–5 TA atherosclerosis was found in 23 (12.6%), 103 (56.6%), 43 (23.6%), 7 (3.8%), and 6 (3.4%) cases respectively. GCS and GCS/PAD decreased as the ultrasound stage of TA atherosclerosis increased as compared with the control group: 9.2% and 15.3 for the control group; stage 1, 5.6% and 8.9 ($p<0.001$); stage 2, 4.1% and 5.9 ($p<0.001$); stage 3, 4% and 5.8 ($p<0.001$); stage 4, 3.7% and 4.9 ($p<0.01$); and stage 5, 2.6% and 3.3 ($p<0.01$), respectively. ROC analysis showed that GCS ≥5.9% (area under the curve, AUC, 0.94±0.03; $p<0.001$) and GCS/PAD ≥11.4 (AUC, 0.97±0.02; $p<0.001$) were predictors of intact TA. Also, GCS ≤4.85% (AUC, 0.82±0.04; $p<0.001$) and GCS/PAD ≤8.06 (AUC, 0.87±0.03; $p<0.001$) were predictors of hemodynamically significant TA atherosclerosis (stages 3–5). GCS ≤4.05% (AUC, 0.62±0.04; $p=0.007$) and GCS/PAD ≤5.95 (AUC, 0.61±0.04; $p=0.018$) were predictors of hemodynamically significant (>50%) stenosing atherosclerosis of at least one CA. Furthermore, GCS ≤3.75% (AUC, 0.67±0.07; $p=0.039$) and GCS/PAD ≤5.15 (AUC, 0.64±0.07; $p=0.045$) were predictors of severe and advanced coronary atherosclerosis (SYNTAX Score ≥22).
Conclusion	GCS and GCS/PAD are new diagnostic markers of structural and functional disorders of TA in atherosclerosis of various grades. GCS and GCS/PAD are independent predictors of high-grade TA atherosclerosis (stages 3–5) with GCS/PAD demonstrating the highest level of significance. GCS and GCS/PAD are non-invasive predictors of severe and advanced CA atherosclerosis.

Keywords	Thoracic aorta; atherosclerosis; 2D speckle-tracking; transesophageal echocardiography; global circumferential strain
For citations	Vrublevsky A.V., Boshchenko A.A., Bogdanov Yu.I., Saushkin V.V., Shnaider O.L. Structural and Functional Disturbances of the Thoracic Aorta in Atherosclerosis of Various Gradations. Kardiologiia. 2023;63(11):64–72. [Russian: Врублевский А.В., Бощенко А.А., Богданов Ю.И., Саушкин В.В., Шнайдер О.Л. Структурно-функциональные нарушения грудного отдела аорты при атеросклерозе различных градаций. Кардиология. 2023;63(11):64–72].
Corresponding author	Vrublevsky A. V. E-mail: avr@cardio-tomsk.ru

Introduction

Physicians, medical imaging experts, and pathophysiologists have not lost interest in evaluating atherosclerosis-related abnormalities in elastic and tonic characteristics of the thoracic aorta [1–4]. Elastic aortic compression chamber (ACC) acts as a powerful pulse wave damper – it converts the left ventricular (LV) ejection kinetic energy into the aortic wall strain energy, which allows reserving end-systole cardiac ejection (the Windkessel effect) and thus ensures continuous balanced systolic-diastolic blood flow through the entire aorta, coronary and peripheral arteries [5]. Atherosclerosis causes structural and functional abnormalities in the aortic wall, alters its strain characteristics, which is accompanied by a gradual loss of elastic and tonic properties and an increase in the aortic wall stiffness [1, 2, 5].

ISSN 0022-9040. Kardiologiia. 2023;63(11). DOI: 10.18087/cardio.2023.11.n2315

Ultrasound and X-ray/tomography examinations are widely used in clinical practice to assess the elastic and tonic properties of the aorta and major peripheral arteries [2–4, 6]. However, transesophageal echocardiography (TEE) is a unique non-invasive technique to estimate the degree of structural and functional abnormalities in the aortic wall due to reproducible clear grayscale transverse imaging of the descending aorta in a standard point at a depth of 25–30 cm from the incisors with the possibility of layer differentiation. That is this technique as an inexpensive model to analyze the elastic and tonic properties of the aortic wall at baseline and over time without subjecting patients to radiation exposure.

In our previous study [5] based on a large clinical material (237 patients with chronic coronary artery disease (CAD)) using two-dimensional (2D) multiplanar TEE, we observed during the progression of the atherosclerotic process that the thoracic aorta lost its elastic and tonic properties, passively dilated, turning into a rigid, hydrodynamically inert tube with a thickened wall and a low amplitude of systolic excursions. However, our study was limited to the determination only local elasticity and stiffness between two preset points of the aortic cross-section in M-mode without assessing the global circumferential systolic strain of the aortic wall. In our opinion, this prevents from seeing a completer and more objective picture of the elastic, tonic and strain properties of the ACC wall. Moreover, all calculated parameters of local elasticity and stiffness depend on systemic blood pressure (BP).

The global circumferential strain of the thoracic aorta and major peripheral arteries are estimated using 2D speckle tracking echocardiography [2, 4, 7, 8] based on a quantitative analysis of the speckle movement in the grayscale image, which are generated by the interaction of the ultrasound beam with the vascular wall tissues. This is a non-Doppler, angle-independent technique that allows quantifying the integral strain characteristics of the vascular wall based on a well-known and clinically proven ultrasound model of the LV along the short axis to assess the circumferential and radial myocardial strain [2, 7, 9]. In the experimental study, Petrini et al. [10] used a thoracic aorta phantom to show a statistically significant relationship ($r = 0.97$; $p<0.01$) between the circumferential strain parameters obtained by 2D speckle-tracking TEE and sonomicrometry data indicating a high accuracy of the technique in quantifying the aortic wall strain characteristics.

Objective

Examine the global aortic circumferential strain in the normal condition and in atherosclerosis of various grades and define its role in the prediction of structural and functional abnormalities of the thoracic aorta and coronary atherosclerosis.

Material and Methods

This study is a continuation of the analysis of the previously studied patient sample described in our article [11]. A total of 182 patients with typical or suspected angina pectoris were examined – 105 males and 77 females, mean age 62.4 ± 7.5 years – referred for diagnostic coronary artery angiography (CAG), repeat coronary stenting, or coronary artery bypass grafting surgery. Clinical characteristics of patients are provided in Table 1. The control group included 11 healthy volunteers – all males, mean age 42.7±5.3 years – with no risk factors and signs of cardiovascular diseases shown during the examination. Most female subjects refused to undergo this examination. Those who underwent screening TEE turned out to have thoracic aortic atherosclerosis and were excluded from the control group. Absolute contraindications to TEE, atrial fibrillation, frequent extrasystole, valvular disorders, cardiomyopathy, left ventricular ejection fraction (LVEF) < 50%, and patient's refusal from the study were the exclusion criteria.

Multiplanar 2D TEE was performed on an empty stomach using expert-grade IE33 xMatrix and Epiq 7G ultrasound diagnostic systems with X7-2t and X8-2t transesophageal probes. Esophageal intubation was performed in the patient's left lateral position after topical oropharyngeal mucosa anesthesia (10% lidocaine spray). The ascending aorta, accessible aortic arch, and the entire descending aorta were studied using xPlane scanning [12]. The condition of the aortic valve and the degree (1–4) of aortic regurgitation were assessed. Blood flow was recorded in the LV outflow tract in the pulse-wave Doppler mode. A series of videos were recorded on the hard disk of the device and later processed off-line in the QLab workstation. During the examination, electrocardiogram (ECG) was synchronously recorded in the modified lead II and systolic (SBP; mm Hg) and diastolic blood pressure (DBP; mm Hg) was measured in the right arm by the oscillometric method with the M2 Basic automatic sphygmomanometer. Pulse BP (PBP; mm Hg) was calculated as PB = SBP – DBP.

The height of each atheroma was measured, and the total number of thoracic atherosclerotic plaques was determined. According to the 2015 guidelines of the American Society of Echocardiography (ASE) and the European Association for Cardiovascular Imaging (EACVI) [12], five stages of thoracic aortic

Table 1. Clinical characteristics of the patients examined

Parameter	Value
Sample size, n	182
Male, n (%)	105 (57.7)
Female, n (%)	77 (42.3)
Mean age, years	62.4 ± 7.5
Coronary artery disease, n (%)	173 (95.1)
Postinfarction cardiosclerosis, n (%)	62 (34.1)
History of coronary artery stenting, n (%)	58 (31.8)
Arterial hypertension, n (%)	168 (92.3)
History of stroke or transient ischemic attack, n (%)	12 (6.6)
Chronic kidney disease stage 3–5 (creatinine clearance < 60 mL/min/m^2), n (%)	42 (23.1)
Obesity (BMI ≥ 30 kg/m^2), n (%)	73 (40.1)
Type 2 diabetes mellitus or impaired glucose tolerance, n (%)	36 (19.8)
Smoking, n (%)	49 (26.9)
Dyslipidemia, n (%)	176 (96.7)
Carotid stenosis < 50 %, n (%)	134 (72.5)
Carotid stenosis ≥ 50 %, n (%)	16 (8.8)
Femoral stenosis < 50 %, n (%)	94 (51.6)
Femoral stenosis ≥ 50 %, n (%)	9 (4.9)
Treatment	
• ASA, n (%)	165 (90.6)
• Anticoagulants, n (%)	33 (18.2)
• Lipid-lowering therapy, n (%)	177 (97.3)
• Beta blockers, n (%)	150 (82.4)
• Nitrates, n (%)	9 (4.9)
• Calcium channel blockers, n (%)	91 (50)
• ACE inhibitors or ARBs, n (%)	152 (83.5)
• Aldosterone receptor antagonists, n (%)	8 (4.4)

BMI, body mass index; ASA, acetylsalicylic acid; ACE, angiotensin-converting enzyme; ARB, angiotensin II receptor blocker.

atherosclerosis are distinguished: stage 1 – an increase in intima-media thickness (IMT) < 2 mm; stage 2 – local or diffuse increase in IMT of 2–3 mm (small atheromas); stage 3 – atheromas >3–5 mm high without mobile or ulcerogenic components; stage 4 – atheromas >5 mm high without mobile or ulcerogenic components; stage 5 – atheromas of any height with a mobile or ulcerogenic component.

For 2D speckle tracking imaging of the thoracic aorta, a grayscale cross-section of the proximal descending aorta was obtained at a depth of 25–30 cm from the incisors at an optimal frame rate (53–60 Hz), outside the atherosclerotic plaque area, with a clear intima media contour and adventitia (Central figure). Peak systolic Lagrangian global circumference strain (GCS; %) was calculated using a short axis LV model [7]. For this purpose, the inner contour of the area of interest on the intima-media complex surface and the outer contour on the outer border of the adventitia were traced in the most accurate manner. According to this model, the aortic cross-section was divided into 6 conditional segments. The software module calculated local strain in each segment, summed up, and produced global circumferential strain (Central figure).

Aortic valve closure time calculated in the Doppler mode by the blood flow spectrum in the LV outflow tract was programmed manually. The software automatically calculated the time to peak systolic circumferential strain (ms) and the change in aortic cross-sectional area (%) during the cardiac cycle. Peak systolic Lagrangian global circumference strain normalized to pulse BP (GCS/PBP × 100) and aortic wall stiffness index β_2 proposed by Oishi et al. were then calculated using the formula:

$$\ln (SBP/DBP)/GCS \times 100.$$

IMT was measured in the same cross section at end diastole in at least three conditional segments and the mean value was calculated. The intima-media complex with a clear and even contour <1 mm thick was considered normal [11].

Then a cross section of the descending aorta was performed at the same point in M-mode. The interintimal end systolic diameter (Ds, cm) was measured at the end of the T wave and the end diastolic diameter (Dd, cm) was measured at the peak of the R wave. The following indicators were also calculated: systolic excursion (Ds – Dd; cm), a change in the diameter during the cardiac cycle

$$(Ds - Dd/Ds) \times 100\ (\%),$$

elasticity,

$$2\times (Ds - Dd)/(Dd\times PBP)\ (cm^2\times dyn^{-1}\times 10^{-6})$$

and aortic wall stiffness index β_1 proposed by Hirai et al. using the formula:

$$\ln (SBP/DBP)/(Ds - Dd/Dd).$$

Millimeters of mercury were converted to dyn according to the formula:

$$(10\times PBP)/0.0075\ [5].$$

All patients underwent CAG. Stenosis was considered anatomically significant in coronary artery narrowing >50% in diameter. The number of involved coronary arteries was estimated. Total atherosclerotic lesion was calculated according to the SYNTAX score in 122 (67.1%) patients without coronary stents and coronary artery bypass grafts [15].

Statistical data analysis was carried out in Statistica 10.0 and SPSS Statistics 26.0. The nature of distribution was determined using the Shapiro-Wilk test. Given the non-normal distribution of the sample, the data were presented as the medians and quartiles (Me [Q1;

ISSN 0022-9040. Kardiologiia. 2023;63(11). DOI: 10.18087/cardio.2023.11.n2315

Central Illustration. Short-axis section of the descending aorta in 2D speckle tracking transesophageal echocardiography

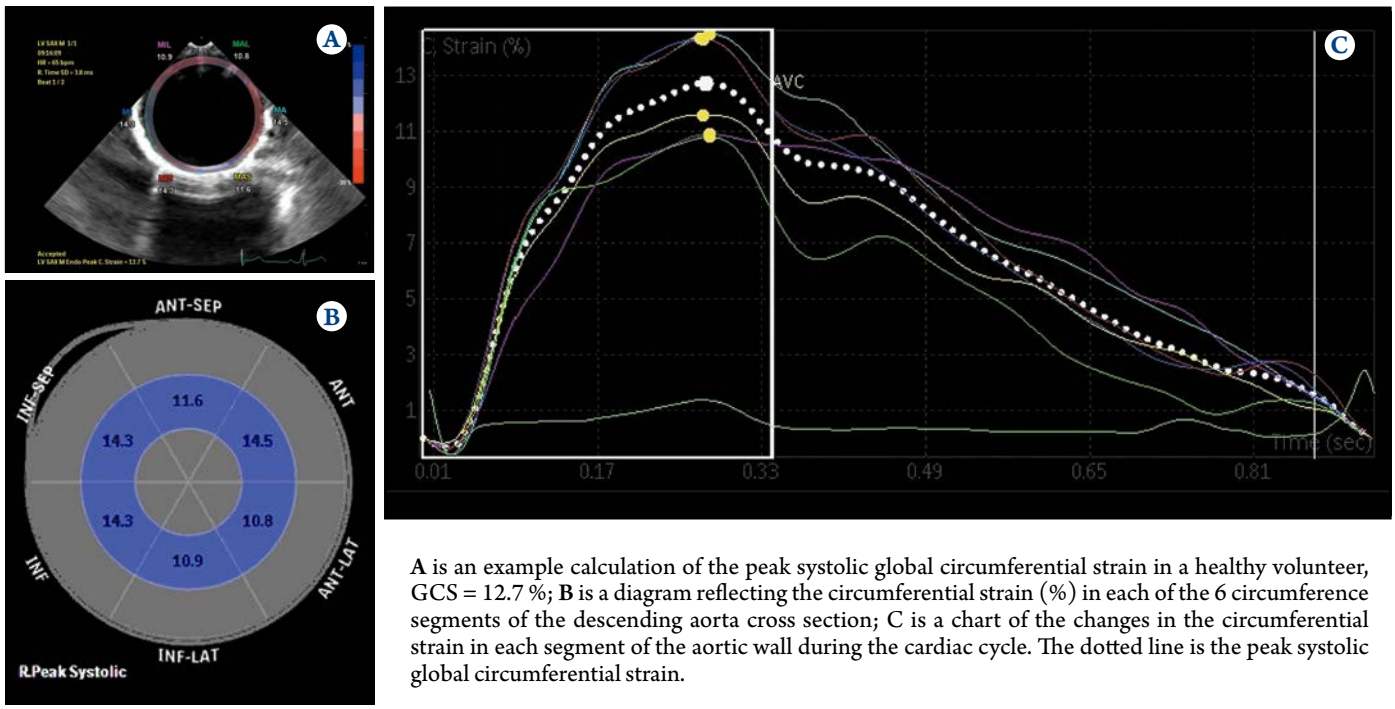

A is an example calculation of the peak systolic global circumferential strain in a healthy volunteer, GCS = 12.7 %; **B** is a diagram reflecting the circumferential strain (%) in each of the 6 circumference segments of the descending aorta cross section; C is a chart of the changes in the circumferential strain in each segment of the aortic wall during the cardiac cycle. The dotted line is the peak systolic global circumferential strain.

Q3]). Intergroup comparisons were evaluated using the Kruskal-Wallis test. Posterior pairwise comparisons were made between the groups using the Holm test. The relationship of aortic strain indicators with clinical, morphometric, and functional characteristics was assessed using the Spearman rank correlation coefficient. Binary univariate and multivariate logistic regression and ROC analysis were used to determine the role and threshold values of GCS and GCS/PBP in the prediction of the ultrasound stage of thoracic aortic atherosclerosis and stenosing coronary artery atherosclerosis. The area under the characteristic curve (AUC) and the 95% confidence interval (CI) were calculated in the ROC analysis.

Results

No ultrasound signs of thoracic aortic atherosclerosis were found in the control group. Atherosclerosis of the thoracic aorta stage 1–5 was detected in 23 (12.6%), 103 (56.6%), 43 (23.6%), 7 (3.8%), and 6 (3.4%) of 182 patients, respectively. Thus, all 193 examined patients were divided into 6 subgroups depending on the ultrasound stage of thoracic aortic atherosclerosis.

Changes in the values of systemic BP, IMT, the total number of atherosclerotic plaques, morphometry, elasticity, stiffness, and strain of the thoracic aorta depending on the ultrasound stage of thoracic aortic atherosclerosis is presented in Table 2.

In general, it was found in the subgroups that aortic wall elasticity and strain decreased statistically significantly, and stiffness and remodeling increased with higher ultrasound stage of thoracic aortic atherosclerosis compared with the control group.

Direct statistically significant correlation was detected between GCS and GCS/PBP and systolic excursion, changes in diameter and cross-sectional area, local elasticity, and inverse relationship was found with age, presence of arterial hypertension (AH), IMT, the total number of plaques in the thoracic aorta, ultrasound stage of thoracic aortic atherosclerosis, stiffness index β_1, number of coronary arteries with >50% stenosis, and SYNTAX score (Table 3).

Multivariate stepwise logistic regression analysis, including sex, age, body mass index, PBP, heart rate, presence or absence of dyslipidemia, AH, diabetes mellitus, smoking, and the parameters of aortic wall elasticity and stiffness, showed aortic wall strain indicators GCS and GCS/PBP and local elasticity and stiffness have an independent diagnostic significance for the prediction of significant atherosclerotic changes in the thoracic aorta stage 3–5 (Table 4). Moreover, the ROC analysis found that GCS ≥ 5.9% is a predictor of the intact thoracic aorta with an 80% sensitivity and an 87% specificity (AUC 0.94 ± 0.03; 95% CI 0.88–0.99; p<0.001). As for GCS/PBP, such value was ≥ 11.4 with a 90% sensitivity and a 93% specificity (AUC 0.97±0.02; 95% CI 0.95–0.99; p<0.001). Moreover, GCS ≤ 4.85% was found to be a predictor of hemodynamically significant atherosclerotic changes in the thoracic aorta (stage 3–5) with a 72% sensitivity and a 74% specificity

Table 2. Structural and functional changes in the thoracic aorta and systemic blood pressure depending on the ultrasonic stage of atherosclerosis

Parameter	Ultrasonic stage of thoracic aortic atherosclerosis						Kruskal-Wallis test	Posterior comparisons using Holm's test				
	0, normal (n = 11)	Group 1 (n = 23)	Group 2 (n = 103)	Group 3 (n = 43)	Group 4 (n = 7)	Group 5 (n = 6)		p_{0-1}	p_{0-2}	p_{0-3}	p_{0-4}	p_{0-5}
SBP, mm Hg	134 [123; 148]	137 [123; 154]	151 [136; 168]	148 [137; 163]	151 [138; 146]	158 [132; 179]	H = 15.08; p = 0.010	> 0.05	< 0.01	< 0.05	< 0.05	< 0.05
DBP, mm Hg	78 [75; 84]	77 [71; 85]	77 [71; 85]	74 [66; 88]	74 [67; 96]	71 [51; 92]	H = 2.86; p = 0.721	> 0.05	> 0.05	> 0.05	> 0.05	> 0.05
PBP, mm Hg	55 [45; 60]	60 [45; 72]	73 [60; 85]	74 [64; 85]	76 [61; 85]	87 [75; 93]	H = 27.63; p < 0.001	> 0.05	< 0.001	< 0.001	< 0.01	< 0.01
Total number of atherosclerotic plaques	No plaques found	No plaques found	3 [2; 4]	5 [4; 6]	5 [4; 6]	6 [5; 7]	H = 91.91; p < 0.001	—	—	p_{2-3} <0.001	p_{2-4} <0.001	p_{2-5} <0.01
IMT, cm	0.08 [0.08; 0.09]	0.107 [0.106; 0.111]	0.116 [0.11; 0.125]	0.132 [0.12; 0.138]	0.136 [0.123; 0.143]	0.144 [0.139; 0.151]	H = 88.53; p < 0.001	< 0.001	< 0.001	< 0.001	< 0.001	< 0.01
End-systole dimension, cm	2.2 [2.1; 2.3]	2.4 [2.3; 2.7]	2.4 [2.2; 2.6]	2.5 [2.2; 2.6]	2.4 [2.0; 2.5]	2.6 [2.4; 2.8]	H = 7.29; p = 0.199	> 0.05	> 0.05	> 0.05	> 0.05	> 0.05
End-diastole dimension, cm	1.9 [1.8; 2.1]	2.2 [2.1; 2.5]	2.2 [2.0; 2.4]	2.3 [2.0; 2.5]	2.3 [1.8; 2.3]	2.5 [2.3; 2.7]	H = 12.15; p = 0.033	< 0.05	< 0.05	< 0.01	< 0.05	< 0.05
Change in dimension, %	10 [8.7; 15.5]	8.3 [7.4; 8.7]	8 [6.6; 9.4]	7.5 [4.3; 9.1]	5.6 [4.3; 6.9]	4.3 [3.8; 5.7]	H = 21.71; p < 0.001	< 0.01	< 0.01	< 0.001	< 0.05	< 0.01
Change in cross-sectional area, %	16 [12.3; 20.3]	12.1 [8.5; 14]	8.5 [5.2; 11.6]	7.6 [2.7; 12.3]	5.6 [3.2; 8.2]	4.1 [2.4; 6.3]	H = 29.95; p < 0.001	< 0.01	< 0.001	< 0.001	< 0.01	< 0.01
Systolic excursion, cm	0.3 [0.2; 0.4]	0.2 [0.2; 0.2]	0.2 [0.2; 0.2]	0.2 [0.1; 0.2]	0.1 [0.1; 0.2]	0.1 [0.1; 0.15]	H = 14.93; p = 0.011	< 0.05	< 0.01	< 0.05	< 0.05	< 0.01
Elasticity, $cm^2 \cdot dyn^{-1} \times 10^{-6}$	3.2 [2.6; 4.3]	2.3 [1.8; 2.6]	1.7 [1.3; 2.4]	1.5 [0.9; 2]	1.2 [0.9; 1.6]	0.7 [0.6; 1.3]	H = 38.08; p < 0.001	< 0.01	< 0.001	< 0.001	< 0.01	< 0.01
Hirai stiffness index β_1	4.6 [3.1; 5.3]	6.6 [5.5; 7.4]	8.6 [5.9; 9.7]	10.8 [7.1; 14.3]	12.7 [6.9; 15.2]	17.1 [13.4; 23.9]	H = 38.82; p < 0.001	< 0.001	< 0.001	< 0.001	< 0.01	< 0.01
Peak global circumferential strain, %	9.2 [6.0; 10.7]	5.6 [4.5; 6.6]	4.1 [3.1; 5]	4 [2.8; 5]	3.7 [2.9; 4.3]	2.6 [1.5; 3.9]	H = 39.69; p < 0.001	< 0.001	< 0.001	< 0.001	< 0.01	< 0.01
Peak global circumferential strain/PBP	15.3 [11.6; 21.4]	8.9 [6.6; 11.2]	5.9 [4.1; 7.5]	5.8 [3.8; 8.3]	4.9 [4.0; 7.7]	3.3 [2.3; 4.9]	H = 49.02; p < 0.001	< 0.001	< 0.001	< 0.001	< 0.01	< 0.01
Time to peak systolic strain, ms	40 [33; 59]	337 [256; 398]	332 [271; 408]	371 [329; 394]	414 [389; 437]	557 [526; 587]	H = 33.01; p < 0.001	< 0.001	< 0.001	< 0.001	< 0.01	< 0.01
Oishi stiffness index β_2	5.6 [4.7; 8.1]	10.9 [8.4; 14.4]	17.3 [12.3; 22.2]	18.7 [12.4; 24.7]	20.2 [11.2; 27.8]	31.1 [16.4; 39.5]	H = 49.38; p < 0.001	< 0.001	< 0.001	< 0.001	< 0.01	< 0.01

β_2, Oishi stiffness index (adapted from [13]); β_1, Hirai stiffness index (adapted from [14]).

(AUC 0.82±0.04; 95% CI 0.75–0.89; p<0.001). As for GCS/PBP, it was ≤ 8.06 with a 76% sensitivity and a 78% specificity (AUC 0.87 ± 0.03; 95% CI 0.81–0.93; p<0.001).

Multivariate stepwise logistic regression analysis revealed showed GCS and GCS/PBP are independent predictors of stenosing coronary artery atherosclerosis (Table 5).

The remaining parameters of interest, including local elasticity and stiffness of the aortic wall according to the M-mode data, did not demonstrate a statistically significant diagnostic value for the prediction of stenosing coronary artery atherosclerosis. Moreover, GCS ≤ 3.75% was found to be a predictor of severe and advanced coronary atherosclerosis (SYNTAX ≥ 22) with a 61% sensitivity and a 65% specificity (AUC 0.67±0.07; 95% CI 0.53–0.81; p<0.039). As for GCS/PBP, it was ≤ 5.15 with a 61% sensitivity and a 60% specificity (AUC 0.64±0.07; 95% CI 0.51–0.78; p=0.045). It was found as an alternative diagnostic criterion that GCS ≤4.05%

ISSN 0022-9040. Kardiologiia. 2023;63(11). DOI: 10.18087/cardio.2023.11.n2315

Table 3. Correlation between the indicators of thoracic aortic strain and clinical, morphometric, and functional characteristics

Parameter	Peak global circumferential strain		Peak global circumferential strain/PBP	
	r	p	r	p
Age	-0.46	< 0.001	-0.55	< 0.001
Arterial hypertension	-0.19	< 0.01	-0.25	< 0.001
IMT	-0.37	< 0.001	-0.38	< 0.001
Systolic excursion	0.46	< 0.001	0.41	< 0.001
Change in dimension	0.48	< 0.001	0.43	< 0.001
Change in cross-sectional area	0.46	< 0.001	0.43	< 0.001
Total number of plaques	-0.37	< 0.001	-0.41	< 0.001
Ultrasonic stage of atherosclerosis	-0.27	< 0.001	-0.33	< 0.001
Elasticity	0.49	< 0.001	0.71	< 0.001
Hirai stiffness index β_1	-0.41	< 0.001	-0.51	< 0.001
Number of coronary arteries with >50 % stenosis	-0.24	< 0.01	-0.22	< 0.05
SYNTAX score	-0.23	< 0.01	-0.21	< 0.05

β_1, Hirai stiffness index according (adapted from [14]).

Table 4. Results of univariate and multivariate logistic regression analysis in the prediction of ultrasonic stage 3–5 of thoracic aortic atherosclerosis

Parameter	Univariate analysis			Multivariate analysis		
	OR	95 %CI	p	OR	95 %CI	p
Age	1.07	1.03–1.12	0.002	1.15	0.31–4.28	0.832
Hirai stiffness index β_1	1.14	1.06–1.23	< 0.001	1.71	1.11–2.63	0.014
Elasticity	0.57	0.51–0.74	0.001	0.62	0.51–0.78	0.002
Peak global circumferential strain	0.79	0.65–0.97	0.024	0.81	0.73–0.87	0.016
Peak global circumferential strain/PBP	0.88	0.79–0.97	0.015	0.63	0.51–0.79	< 0.001
Oishi stiffness index β_2	1.04	1.01–1.07	0.042	0.97	0.81–1.17	0.031

β_2, Oishi stiffness index (adapted from [13]); β_1, Hirai stiffness index (adapted from [14]).

Table 5. Results of univariate and multivariate logistic regression analysis in the prediction of stenosing coronary atherosclerosis > 50 %

Parameter	Univariate analysis			Multivariate analysis		
	OR	95 %CI	p	OR	95 %CI	p
Peak global circumferential strain	0.75	0.61–0.92	0.006	0.76	0.61–0.94	0.011
Peak global circumferential strain/PBP	0.87	0.79–0.96	0.008	0.81	0.69–0.94	0.005

OR, odds ratio; CI, confidence interval.

is a predictor of hemodynamically significant (> 50%) stenosing atherosclerosis of at least one major coronary artery with a 60% sensitivity and a 61% specificity (AUC 0.62 ± 0.04; 95% CI 0.53–0.69; p=0.007). As for GCS/PBP, it was ≤5.95 with a 61% sensitivity and a 62% specificity (AUC 0.61±0.04; 95% CI 0.52–0.68; p=0.018).

Discussion

The indicators of the aortic and arterial wall stiffness are well-known informative predictors of fatal cardiovascular complications, that is why the search for new non-invasive diagnostic markers to assess abnormalities of the elastic and tonic properties of ACC and large elastic vessels in clinical settings is an urgent task of modern ultrasound and X-ray tomography imaging [1–4, 6]. In this regard, the idea of extrapolating the well-known ultrasound model for determining the LV circumferential strain to the cross section of tubular elastic structures, particularly the aorta, using the 2D speckle tracking echocardiography seems original and interesting with regard to blood circulation

mechanics. The main advantage of 2D speckle tracking estimation of the aortic wall circumferential strain is obtaining integral strain values throughout the entire circumference of the aorta as a mean of 6 different segments, in contrast to the previously proposed ultrasound models in M-mode, in which the elastic and tonic properties were evaluated locally between two points of the longitudinal or cross section [5, 7]. Many researchers applied this idea and method for transthoracic ultrasound of the ascending aorta and obtained interesting results for clinicians. Bu et al. [2] demonstrated a gradual decrease in circumferential strain of the ascending aorta in CAD patients depending on the number of stenotic major coronary arteries compared with subjects without CAD and showed its role in predicting three-vessel coronary disease. At the same time, in our opinion, the calculation of the strain indicators of a 1–2 mm thick aortic wall on the cross sections of the ascending aorta in 15–16 cm from the sensor in transthoracic ultrasound have technical restrictions and errors. In this regard, 2D speckle-tracking transesophageal ultrasound of the thoracic aorta using high-frequency matrix probes located next to the structure of interest is a more promising imaging method from a technical and technological point of view that provides an inexpensive and easily reproducible model for assessing circumferential strain of the aortic wall [4, 7]. Petrini et al. [10] successfully proved this point of view on the thoracic aorta phantom in their experimental study.

We conducted a multiplanar transesophageal ultrasound of the structural and functional changes in the thoracic aorta in atherosclerosis of various grades using speckle tracking technique based on a comprehensive analysis of the ultrasonic stage of atherosclerosis, elasticity, stiffness and circumferential strain of the aortic wall. Our analysis of changes in morphometry, elasticity, stiffness, and circumferential strain of the aortic wall depending on the ultrasonic stage of atheromatosis showed that the progression of the aortic atherosclerotic process is accompanied not only by a gradual loss of its elastic and tonic properties (which confirms the results of our previous studies [5]), but also by a decrease in strain characteristics with further passive dilation and transformation into a rigid, hydrodynamically inert, non-deformable tube with a thickened wall and low amplitude of systolic excursions. The shown gradual remodeling of the thoracic aorta in atherosclerosis of various grades does not generally contradict Bernoulli's theorem [16], which implies that the loss of elastic and tonic properties and the loss of strain characteristics of the aortic wall revealed in this study leads to a more rapid passive dilation of the vessel, decreasing blood flow, and increasing lateral pressure. At the same time, according to Laplace's law [16], the stress on the wall from the blood flow increases with larger diameter, which limits the possibility of its strain and contributes to further dilatation of the vessel. Based on the described abnormalities of the aortic wall mechanics, it should be noted that the atherosclerotic aorta undoubtedly loses the role of the pulse wave damper due to the loss of both elastic and tonic properties and strain characteristics, which causes the aortic blood flow imbalance, as shown by Catapano et al. [6].

The correlation of the above-described pathophysiological mechanisms of gradual failure of the ACC in atherosclerosis of various grades is also confirmed by the inverse correlation of the aortic wall strain indicators with IMT, the total number of atheromas, ultrasonic stage of atherosclerosis, stiffness index, and the direct correlation with changes in diameter, cross-sectional area, amplitude of systolic excursion, and aortic elasticity. It is not surprising that age and the presence of AH are additional factors limiting the elasticity and strainability of the aortic wall in atherosclerosis.

The results of our logistic regression and ROC analyses enable to assert that indicators of the aortic wall circumferential strain, in addition to their role in the pathogenesis of ACC mechanics abnormalities in atherosclerosis, have independent diagnostic value both for the prediction of the ultrasonic norm and the stage of significant atherosclerotic changes in the thoracic aorta. It should be especially emphasized that in multivariate regression analysis, it was GCS/PBP as an integral indicator of the circumferencial strain of the entire aortic wall, given the systemic hemodynamics, which turned out to be the most reliable independent predictor of high-grade thoracic aortic atherosclerosis (stages 3–5). Moreover, the quantitative criterion for the diagnosis of high-grade thoracic aortic atherosclerosis (stage 3–5) was obtained exactly for this indicator (GCS/PBP) in the ROC analysis with the highest sensitivity and specificity.

According to our findings, the circumferential strain of the aortic wall is a new non-invasive predictor of stenosing coronary artery atherosclerosis. It should be noted that in multivariate regression analysis, unlike previously known indicators of local elasticity and stiffness based on the M-mode data, the integral strain characteristics of the aortic wall GCS and GCS/PBP demonstrated an independent role in the prediction of

ISSN 0022-9040. Kardiologiia. 2023;63(11). DOI: 10.18087/cardio.2023.11.n2315

both hemodynamically significant coronary stenosis (>50%) and the severity and prevalence of coronary atherosclerosis in general (SYNTAX ≥ 22).

Thus, we believe that the application of the model of non-invasive estimation of the aortic wall strain characteristics using the 2D speckle tracking echocardiography is certainly of both theoretical and clinical interest in the interpretation of the results of transesophageal ultrasound of the thoracic aorta at screening and over time, diagnosis of early and surrogate markers of coronary and aortic atherosclerosis.

Limitations

Our study had certain limitations. We were forced to exclude from the study subjects with the descending aorta cross sections being beyond the specified sector of the grayscale image at the optimal frame rate (53–60 Hz), which did not allow the software to accurately trace the intimal and adventitious contours of the aortic wall throughout its circumference. Moreover, the study did not include subjects with severe and advanced atheromatosis due to the impossibility to distinguish an area of interest outside of atherosclerotic plaques.

Conclusions

Indicators of the peak systolic global circumferential strain (GCS) of the aorta and the peak systolic global circumferential strain normalized to pulse blood pressure (GCS/PBP) according to 2D speckle tracking transesophageal echocardiography, are new diagnostic markers of structural and functional abnormalities of the thoracic aorta in atherosclerosis of various grades.

GCS and GCS/PBP, elasticity and stiffness indicators are independent predictors of high-grade thoracic aortic atherosclerosis (stages 3–5), with GCS/PBP having the highest level of significance.

Unlike local elasticity and stiffness indicators calculated based on the M-mode data, GCS and GCS/PBP based on 2D speckle tracking transesophageal echocardiography are non-invasive predictors of pronounced and advanced coronary atherosclerosis.

Funding

No funding was received for this study.

No conflict of interest is reported.

The article was received on 10/11/2022

REFERENCES

1. Mitchell GF. Arterial Stiffness in Aging: Does It Have a Place in Clinical Practice?: Recent Advances in Hypertension. Hypertension. 2021;77(3):768–80. DOI: 10.1161/HYPERTENSIONAHA.120.14515
2. Bu Z, Ma J, Fan Y, Qiao Z, Kang Y, Zheng Y et al. Ascending Aortic Strain Analysis Using 2-Dimensional Speckle Tracking Echocardiography Improves the Diagnostics for Coronary Artery Stenosis in Patients With Suspected Stable Angina Pectoris. Journal of the American Heart Association. 2018;7(14):e008802. DOI: 10.1161/JAHA.118.008802
3. Wehrum T, Günther F, Kams M, Wendel S, Strecker C, Mirzaee H et al. Quantification of aortic stiffness in stroke patients using 4D flow MRI in comparison with transesophageal echocardiography. The International Journal of Cardiovascular Imaging. 2018;34(10):1629–36. DOI: 10.1007/s10554-018-1369-2
4. Rong LQ, Kim J, Gregory AJ. Speckle tracking echocardiography: imaging insights into the aorta. Current Opinion in Cardiology. 2020;35(2):116–22. DOI: 10.1097/HCO.0000000000000706
5. Vrublevsky A.V., Boshchenko A.A., Karpov R.S. Complex ultrasound assessment of atherosclerosis of thoracic aorta and coronary arteries. -Tomsk: STT;2007. - 180 p. [Russian: Врублевский А.В., Бощенко А.А., Карпов Р.С. Комплексная ультразвуковая оценка атеросклероза грудного отдела аорты и коронарных артерий. – Томск: STT, 2007. – 180 с]. ISBN 5-93629-268-1
6. Catapano F, Pambianchi G, Cundari G, Rebelo J, Cilia F, Carbone I et al. 4D flow imaging of the thoracic aorta: is there an added clinical value? Cardiovascular Diagnosis and Therapy. 2020;10(4):1068–89. DOI: 10.21037/cdt-20-452
7. Alreshidan M, Shahmansouri N, Chung J, Lash V, Emmott A, Leask RL et al. Obtaining the biomechanical behavior of ascending aortic aneurysm via the use of novel speckle tracking echocardiography. The Journal of Thoracic and Cardiovascular Surgery. 2017;153(4):781–8. DOI: 10.1016/j.jtcvs.2016.11.056
8. Iino H, Okano T, Daimon M, Sasaki K, Chigira M, Nakao T et al. Usefulness of Carotid Arterial Strain Values for Evaluating the Arteriosclerosis. Journal of Atherosclerosis and Thrombosis. 2019;26(5):476–87. DOI: 10.5551/jat.45591
9. Cameli M, Mandoli GE, Sciaccaluga C, Mondillo S. More than 10 years of speckle tracking echocardiography: Still a novel technique or a definite tool for clinical practice? Echocardiography. 2019;36(5):958–70. DOI: 10.1111/echo.14339
10. Petrini J, Eriksson MJ, Caidahl K, Larsson M. Circumferential strain by velocity vector imaging and speckle-tracking echocardiography: validation against sonomicrometry in an aortic phantom. Clinical Physiology and Functional Imaging. 2018;38(2):269–77. DOI: 10.1111/cpf.12410
11. Vrublevsky A.V., Boshchenko A.A., Bogdanov Yu.I. Possibilities and limitations of three-dimensional transesophageal echocardiography in the diagnosis of thoracic aorta atherosclerosis. Kardiologiia. 2019;59(10S):22–30. [Russian: Врублевский А.В., Бощенко А.А., Богданов Ю.И. Возможности и ограничения трехмерной чреспищеводной эхокардиографии в диагностике атеросклероза грудного отдела аорты. Кардиология. 2019;59(10S):22–30]. DOI: 10.18087/cardio.n692
12. Goldstein SA, Evangelista A, Abbara S, Arai A, Asch FM, Badano LP et al. Multimodality Imaging of Diseases of the Thoracic Aorta in Adults: From the American Society of Echocardiography and the European Association of Cardiovascular Imaging. Journal of the American Society of Echocardiography. 2015;28(2):119–82. DOI: 10.1016/j.echo.2014.11.015
13. Oishi Y, Mizuguchi Y, Miyoshi H, Iuchi A, Nagase N, Oki T. A Novel Approach to Assess Aortic Stiffness Related to Changes in Aging Using a Two-Dimensional Strain Imaging. Echocardiography. 2008;25(9):941–5. DOI: 10.1111/j.1540-8175.2008.00725.x

14. Hirai T, Sasayama S, Kawasaki T, Yagi S. Stiffness of systemic arteries in patients with myocardial infarction. A noninvasive method to predict severity of coronary atherosclerosis. Circulation. 1989;80(1):78–86. DOI: 10.1161/01.CIR.80.1.78
15. Sianos G, Morel M-A, Kappetein AP, Morice M-C, Colombo A, Dawkins K et al. The SYNTAX Score: an angiographic tool grading the complexity of coronary artery disease. EuroIntervention. 2005;1(2):219–27. PMID: 19758907
16. Caro C, Pedley T, Schroter R, Seed W. The mechanics of the circulation. -M.: Mir;1981. - 624 p. [Russian: Каро К., Педли Т., Шротер Р., Сид У. Механика кровообращения. – М.: Мир, 1981. – 624 с]

ISSN 0022-9040. Kardiologiia. 2023;63(11). DOI: 10.18087/cardio.2023.11.n2315